

Mapping Bennu with Sunlight and Lasers: The SPCOLA methods J. H. Roberts¹, O. S. Barnouin¹, R. W. Gaskell², E. E. Palmer², J. R. Weirich², M. Daly³, J. Seabrook³, R. C. Espiritu¹, A. H. Nair¹, M. E. Perry¹, and D. S. Lauretta⁴ ¹Johns Hopkins University Applied Physics Laboratory, 11100 Johns Hopkins Rd., Laurel, MD 20723-6099, ²Planetary Science Institute, 1700 E. Fort Lowell, Tucson, AZ, 85719-2395. ³York University, 4700 Keele Street, Toronto, ON, Canada, M3J 1P3, ⁴Lunar and Planetary Laboratory, University of Arizona, Tucson, AZ. Corresponding Author's Email: James.Roberts@jhuapl.edu

Introduction: Two instruments on OSIRIS-REx enable independent determination of topography. The OSIRIS-REx Camera Suite (OCAMS) includes the wide-angle MapCam and the narrow-angle PolyCam. By performing stereophotoclinometry (SPC) on these images returned by these cameras, we can construct slope and albedo maps or "maplets" of small patches of the surface with central control points [1]. The OSIRIS-REx Laser Altimeter (OLA) is a scanning lidar that ranges to the surface and can be used to develop local and global scale topographic maps.

The combination of SPC and OLA, or "SPCOLA" leverages the strengths of both techniques while mitigating their respective weaknesses, and allows us to generate Digital Terrain Models (DTMs) with higher accuracy than would be possible from either data set alone. Here we describe two SPCOLA methods, one in a relatively data-poor environment (e.g., the Preliminary Survey phase) and one when data are plentiful (e.g., Orbital Phase B).

SPC: The strength of SPC is that it provides solutions of topography with accuracies similar to those of the best images used [1–3]. SPC makes use of images in a wide range of viewing geometries, illuminations, and resolutions that can fill in gaps where altimetric data from other sources may not exist. SPC also provides precise control point location for large stereo separation over multiple trajectories and even multiple spacecraft. This technique has been used successfully to characterize the topography of several small bodies, including Eros, Phobos, Mimas, Lutetia, Itokawa, Vesta, comet 67P, Mercury and the Moon [4–12].

OLA: Key strengths of lidar ranging include the ability to operate under any illumination conditions, including in the dark and providing an absolute measure of the range constraint to the surface. This range can be used to derive a control network for SPC. The range improves the knowledge of the spacecraft position and provides constraints for any gravity solution obtained with radio science. OLA is unique from other altimeters, in that it is capable of firing at 100Hz and 10kHz depending on range from the surface. It also possesses a scanning mirror that can span ± 6 degrees. The laser has a 100-200 μ m spot size (depending on range), corresponding to 7 cm spot size in the orbital phase, and an absolute precision of ± 3 cm vertically.

Method 1: "Sparse" data: Because OSIRIS-REx does not arrive at its target until late 2018, we test the

SPCOLA techniques using synthetic data. We use a high resolution "truth" model, which has been previously been generated for the purpose of testing data analysis techniques before flight data are available. This model has 5 cm global resolution for most regions of the asteroids, and >1 cm resolution near a plausible sample site. This "truth model" has been virtually imaged and scanned according to planned trajectory of the real flight system. A series of shape models has been constructed from these synthetic images [13].

During the Preliminary Survey (PS) phase we have good MapCam image coverage as well as PolyCam images from Approach. However, the OLA data is relatively sparse; and our first method is designed to make the most of what OLA data is available. We use OLA ranges to constrain positions of critical images and build landmarks and a shape model around those constraints.

We take a 75-cm SPC shape model based on (synthetic) images from Approach and PS phases and identify a few (4–6) key MapCam images (~ 50 cm/px resolution) taken at locations distributed around the asteroid (Fig. 1.) We then find OLA shots taken at the same time as these critical images, and use those as the absolute ranges for these images. We then generate new spacecraft-object vectors for these images, precisely locating

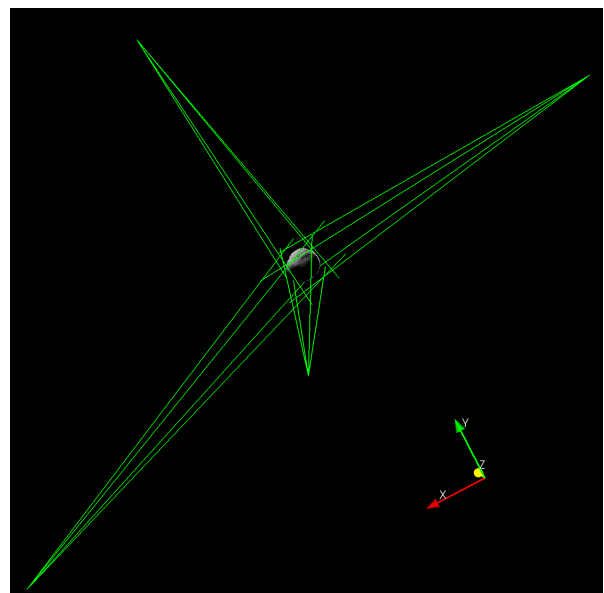


Figure 1: MapCam images projected on to shape model of Bennu. Green lines show the frustums of each; the s/c is at the apex at the time each image was taken.

them relative to the Bennu center of figure. We then rebuild the SPC landmarks with all available images, tied to the critical images.

The critical images pinned by OLA are shifted ~ 20 cm in the $-z$ -direction from the SPC nominal solution. The position uncertainties of the lidar-constrained key images (~ 50 cm) are much smaller than the nominal SPC solution (few m for this phase). The resulting landmark maps are shifted by a few cm. The differences in the shape models between SPC and this form of SPCOLA are shown in Figure 2.

Method 2: Plentiful data. In Orbital Phase B (OB), we are not as data constrained as we are earlier in the mission. Here, our approach is to take maps created independently using SPC and OLA and combine them to develop higher-order data products.

We process the OLA data into a format compatible with the SPC utilities. We take the synthetic OLA database (including spacecraft navigation errors and instrument noise) for Orbital Phase B [14] and generate a series of 5-cm "mapolas," maps made from the OLA data in the same file format as the SPC maplets. We then use the SPC utilities to bring the mapolas into the existing SPC solution (an SPC shape model with the associated 30-cm maplets). The spacecraft–surface vector of each mapola is adjusted to minimize the misfit between the mapola and images in the same area, and the initially blank albedo field in the mapola is populated from the SPC solution. At this stage, the mapola solution itself is not altered by SPC, only its position. In this way, we have heights for a given region determined independently by both SPC and OLA. Finally, we generate larger "bigmaps" from the mapolas and maplets contained within that region.

Our results are shown in Figure 3. We find that the SPC maplets underestimate heights of blocks and depths of craters, while OLA reproduces block heights more closely, but some spikes (bad data) are not removed. In the SPCOLA solution, the OLA spikes corrected by SPC, and OLA provides absolute range constraints.

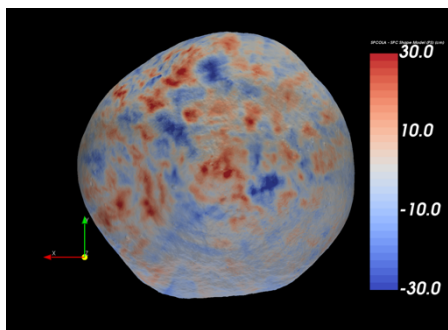


Figure 2: South polar view of PS phase Bennu shape model. The color scale shows difference in elevation (in cm) between the SPCOLA and SPC solutions.

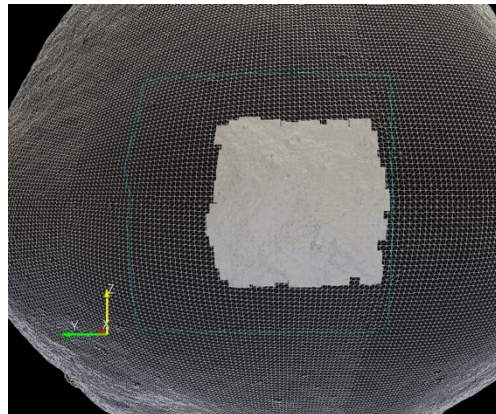


Figure 3: 300 Mapolas mapped onto wireframe Bennu shape model. Square outline indicates boundaries of example bigmap.

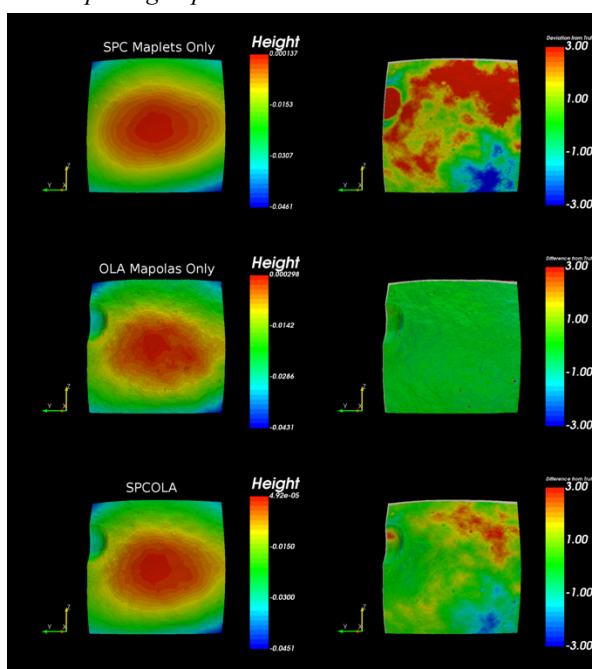


Figure 4: Left column: bigmaps of region outlined in Fig. 3 using maplets (top), mapolas (center) and both (bottom). Scale bar in km. Right column: Deviation (in m) between the bigmap and the truth model.

References: [1] Gaskell, R. W., et al. (2008), *MAPS* 43, 1049-1061. [2] Palmer, E. E. et al. (2016), *Earth Space Sci.* 3, 488–509. [3] Gaskell R.W. et al. (2006) *LPSC* 37, 1876. [4] Gaskell R.W. et al. (2009) *AGU Spring*, #P13A-04. [5] Gaskell R.W. (2011) *LPSC* 42, 1608. [6] Jorda L. et al. (2011) *EPSC-DPS Joint Meeting*, 776. [7] Gaskell R.W. et al. (2012) *DPS*, #209.03. [8] Gaskell R.W. (2014) *DPS*, #209.04. [9] Roberts, J.H. et al. (2014) *MAPS* 49, 1735–1748. [10] Ernst C.M. et al. (2015) *LPSC* 46, 1832. [11] Perry, M.E. et al. (2015) *GRL* 42, 6951–6958. [12] Craft, K. et al. 2017, *LPSC* 48, 2564 [13] Weirich, J.W. et al. (2017) *LPSC* 48, 1700. [14] Perry, M.E. et al. (2017) *LPSC* 48, 2963.